



This is a repository copy of *Transition from propagating polariton solitons to a standing wave condensate induced by interactions*.

White Rose Research Online URL for this paper:
<http://eprints.whiterose.ac.uk/130113/>

Version: Accepted Version

Article:

Sich, M. orcid.org/0000-0003-4155-3958, Chana, J.K., Egorov, O.A. et al. (8 more authors) (2018) Transition from propagating polariton solitons to a standing wave condensate induced by interactions. *Physical Review Letters*, 120. 167402. ISSN 0031-9007

<https://doi.org/10.1103/PhysRevLett.120.167402>

Reuse

Items deposited in White Rose Research Online are protected by copyright, with all rights reserved unless indicated otherwise. They may be downloaded and/or printed for private study, or other acts as permitted by national copyright laws. The publisher or other rights holders may allow further reproduction and re-use of the full text version. This is indicated by the licence information on the White Rose Research Online record for the item.

Takedown

If you consider content in White Rose Research Online to be in breach of UK law, please notify us by emailing eprints@whiterose.ac.uk including the URL of the record and the reason for the withdrawal request.



eprints@whiterose.ac.uk
<https://eprints.whiterose.ac.uk/>

Transition from propagating polariton solitons to a standing wave condensate induced by interactions

M. Sich,^{1,*} J. K. Chana,^{1,2} O. A. Egorov,³ H. Sigurdsson,⁴ I. A. Shelykh,^{4,5} D. V. Skryabin,^{6,5}
P. M. Walker,¹ E. Clarke,⁷ B. Royall,¹ M. S. Skolnick,^{1,5} and D. N. Krizhanovskii^{1,5,†}

¹*Department of Physics and Astronomy, The University of Sheffield, Sheffield, S3 7RH, United Kingdom*

²*Base4 Innovation Ltd, Cambridge, CB3 0FA, United Kingdom*

³*Technische Physik der Universität Würzburg, Am Hubland, 97074, Würzburg, Germany*

⁴*Science Institute, University of Iceland, Dunhagi-3, IS-107 Reykjavik, Iceland*

⁵*Department of Nanophotonics and Metamaterials,*

ITMO University, St. Petersburg, 197101, Russia

⁶*Department of Physics, University of Bath, Bath, BA2 7AY, United Kingdom*

⁷*EPSRC National Centre for III-V Technologies,*

The University of Sheffield, Sheffield, S1 4DE, United Kingdom

We explore phase transitions of polariton wavepackets, first, to a soliton and then to a standing wave polariton condensate in a multi-mode microwire system, bluemediated by nonlinear polariton interactions. At low blue excitation density, we observe ballistic propagation of the multi-mode polariton wavepackets arising from the interference between different transverse modes. With increasing excitation density, the wavepackets transform into single-mode bright solitons due to effects of both inter-modal and intra-modal polariton-polariton scattering. Further increase of the excitation density increases thermalisation speed leading to relaxation of the polariton density from a solitonic spectrum distribution in momentum space down to low momenta with the resultant formation of a non-equilibrium condensate manifested by a standing wave pattern across the whole sample.

Introduction.— Self-organisation of nonlinear waves plays a fundamental role in a wide variety of phenomena, which in many cases have shaped the development of key areas of modern physics. These effects include Bose-Einstein condensation (BEC) [1], spontaneous pattern formation [2], turbulence, solitons [3] and topological defects. Solitons are self-sustained objects characterised by energy localisation in space and time through a balance between nonlinearity and dispersion. They contain a broad spectrum of waves with different energies and momenta. By contrast BEC is characterised by a quasi-homogeneous density distribution in real space and a narrow spectrum in momentum space. Both have been observed in cold atomic gases [4, 5] and polariton systems [6].

In nonlinear optics the interplay between nonlinearity, spatial, and temporal degrees of freedom is particularly interesting. It enables the study of ultra-broadband emission and multi-mode solitons [7] in fibres and BEC-like condensation of classical waves in nonlinear crystals [8]. Both effects arise from scattering between different transverse modes [7, 9]. Describing such complex systems analytically or numerically poses great challenges. Kinetic wave theory and principles of thermodynamics [10, 11] have been used to explain supercontinuum (SC) generation in optical fibres [12], incoherent spectral solitons [13, 14], and polariton condensation [15] while coupled nonlinear Schrödinger equations, which neglect any incoherent wave population, have been used to describe multi-mode solitons [16, 17].

Polaritons in optical microresonators, where strong

exciton-photon hybridisation enables giant $\chi^{(3)}$ optical nonlinearity [18, 19], form a unique laboratory for the study of nonlinear collective phenomena, including BEC and polariton lasing [20–23], self-organisation through multiple polariton-polariton scattering [24], quantised vortices [25, 26] and solitons [27–29]. While in planar 2D microcavities polariton-polariton scattering usually occurs between the states residing in a single band formed by the lower polariton branch [30], a range of scattering channels opens up in laterally confined systems, such as microcavity wires (MCWs) [31, 32] where nonlinear interactions can mix between different transverse polariton modes [33]. Theoretically this mixing can lead to competition between modes of different parity and formation of parity switching waves and parity solitons under static nonresonant excitation [34, 35].

In this letter we demonstrate, both experimentally and numerically, an evolution of a multimode polariton system between phases of contrasting properties: multimode wavepacket \rightarrow soliton \rightarrow soliton doublet \rightarrow dynamic condensate. The crucial ingredients for the observed evolution are the specific shape of the microcavity polariton dispersion, arising from strong exciton-photon coupling, where the sign of the polariton effective mass changes from positive to negative with increasing momentum, the existence of multiple transverse modes, and strong polariton nonlinearities. In the nonlinear regime polariton-polariton interactions redistribute the particles between several transverse lower polariton modes. At intermediate powers, propagating bright single- and double-peak solitons form, which are characterised by a dominant

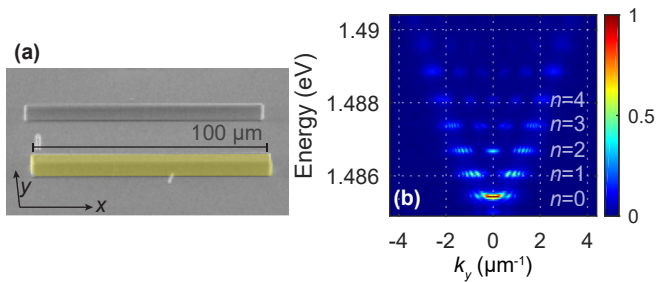


FIG. 1. (a) SEM image of the sample with etched microwires. The $8 \mu\text{m}$ by $100 \mu\text{m}$ wire is shaded in yellow. (b) Energy-momentum dispersion of the lower polariton branch measured across the wire, along the y -axis, showing different energy modes arising from lateral photonic confinement. The fine modulation of the mode dispersions arises from interference due to reflection from the polished side of the substrate [36].

occupation in a finite range of non-zero momenta just above the point of inflexion of the dispersion curve. At even stronger excitation, cascading polariton-polariton and polariton-exciton scattering leads to relaxation of the polariton density from the solitonic mode to lower momenta, and a non-equilibrium analogue of BEC is formed, characterised by a standing wave pattern. It is possible to achieve this quasi-thermalised state because the long polariton lifetime of $\simeq 30$ ps and very strong Kerr-like polariton nonlinearity (leading to interaction times much shorter than the lifetime) allow efficient redistribution of polariton density. These observations are realised in a $100 \mu\text{m}$ -long MCW.

To compare the experimental results with theoretically expected behaviour we used the generalised Gross-Pitaevskii equation (see, *e.g.*, [37]) with an additional phenomenological nonradiative excitonic decay accounting for decoherence. Details of the modelling are given in the Supplemental Materials [38]. Previously, conservative bright polariton solitons have been reported in a narrow and long MCW [39] where only the ground polariton transverse mode was excited and multimode evolution, mode competition, or standing wave condensation were not observed. In multimode polariton systems, condensation [31, 32] and ballistic propagation [40] have only been reported separately. In optical fibres, where typically solitons and supercontinuum generation are observed (see *e.g.* [41]), spectral narrowing [42] and spectral condensation in ultra-long fibre lasers [43] were reported, but again a transition from soliton to condensate behaviour was not observed.

Results. — Our sample is a $3\lambda/2$ microcavity with 3 InGaAs quantum wells (10 nm thick, 4% Indium), and was previously described in the Ref. [44]. Distributed Bragg mirrors are GaAs/AlGaAs (85% Al) with 26 (23) repeats on the bottom (top) mirror. The Rabi splitting and polariton lifetime are $\simeq 4.12$ meV and $\simeq 30$ ps. The top mirror was partially etched defining $100 \mu\text{m}$ -

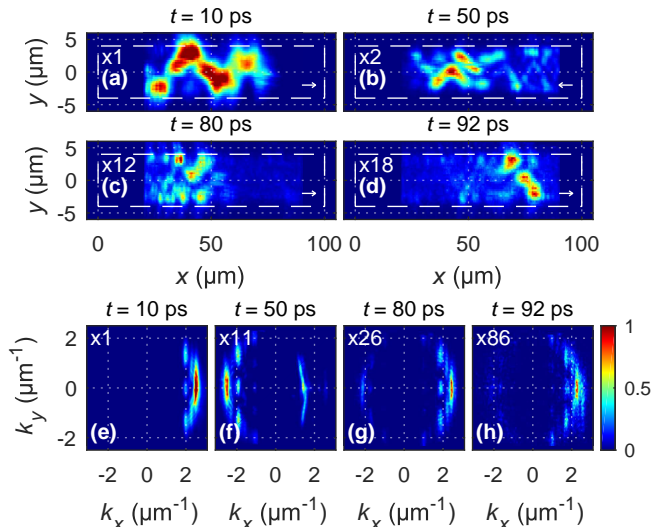


FIG. 2. Low power, $P_1 = 90 \mu\text{W}$, emission characterisation. (a-d) Reconstructed real-space images of the polariton pulse propagating in the MCW at different times. White dashed rectangles show the outline of the MCW. Arrows in lower right corners indicate the direction of travel of the pulses. (e-h) are the corresponding snapshots of the momentum space at the same times as (a-d) respectively. All pseudo-colour scales are linear 0 to 1, and numbers in top-right corners of each panel are intensity scaling factors applied to data for each panel.

long, $8 \mu\text{m}$ wide mesas (Fig. 1(a)). The lateral confinement of the photonic mode generates discrete energy levels labelled as $n = 0, 1, 2, \dots$ (where n is the number of nodes in the photon field distribution across the wire), which can be seen in the far-field polariton photoluminescence (PL) under a low-power non-resonant excitation (Fig. 1(b)). The ground, $n = 0$, photonic mode is detuned by $\simeq -4.07$ meV from the exciton at 1490meV .

We applied a quasi-resonant pulsed excitation laser at an angle of incidence relative to the sample top surface corresponding to $k_x \simeq 2.4 \mu\text{m}^{-1}$ and $k_y \simeq 0$. The excitation beam was spectrally-filtered to approx. 5-7 ps duration FWHM (corresponding to $\simeq 0.3$ meV energy width) and focused into a spot size of $\simeq 20 \mu\text{m}$ close to one end of the wire. The finite width of the pulse in momentum, $\Delta k_x \simeq 0.4 \mu\text{m}^{-1}$, as well as Rayleigh scattering from the edges of the etched MCW enables efficient excitation of three ($n = 0, 1, 2$) transverse lower polariton modes (Fig. 2(e)). We start with the lowest excitation power, $P_1 = 90 \mu\text{W}$ (Fig. 2), corresponding to $P_0 = 1$ meV μm^{-2} in the numerical modelling [38], when polariton-polariton interactions are negligible. The excited polariton modes have different group velocities in the range of $\sim 1\text{-}3 \mu\text{m}/\text{ps}$, which, in addition to polariton group velocity dispersion (GVD) of each transverse polariton mode, leads to spreading of the pulse in real-space. The interference between the transverse modes also results

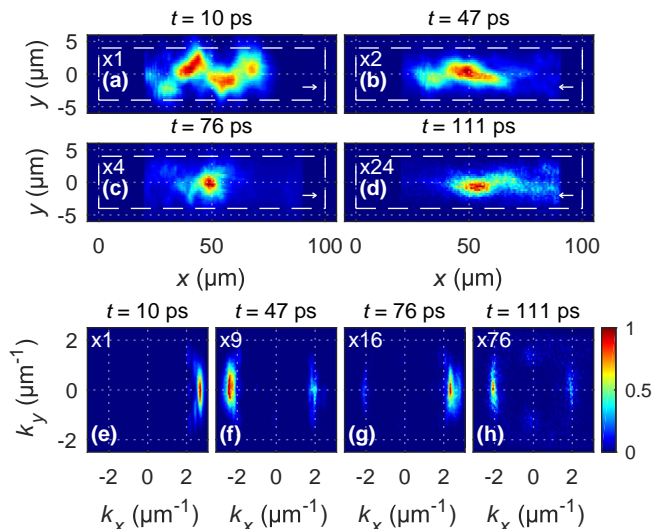


FIG. 3. Medium power, $P_2 = 540 \mu\text{W}$, emission characterisation for different times. Labelling is the same as in Fig. 2

in a visible 'snaking' (see Ref. [40]) of the pulse in real space (Fig. 2(a), and in the theory Figs. S3(a-c)) with frequency $\omega_s = \hbar(k_{x,n=0}^2 - k_{x,n=1}^2)/2m$, see (S4).

The long polariton lifetime allows us to observe several cycles of the pulse moving back and forth along the wire. Fig. 2 provides several snap-shots of this process showing the real-space images and the corresponding k-space distributions. Within $\simeq 30$ ps after the excitation, the front of the pulse quickly reaches the end of the wire, where it is elastically reflected backwards so that the momentum of polariton emission changes its sign (Fig. 2(f))[45]. The same is seen in modelling in Figs. S2(f,j). During reflections from the ends of the wire, polariton modes of higher orders, *i.e.* $n = 3$ and 4 , are also populated through the elastic scattering of the pulse from imperfections (Figs. 2(f-h)). The interference between low- and high-order modes enhances the overall pulse spreading and produces more complex real-space patterns (Figs. 2(b,c,d)). Overall, at the low pump power the momentum emission associated with different modes is almost the same at $\simeq 10$ and $\simeq 90$ ps, confirming low efficiency of polariton relaxation in energy-momentum space due to weak interactions with phonons, which is also reproduced in our modelling (see Fig. S3 of the SM [38]).

At intermediate power, $P_2 = 540 \mu\text{W}$, corresponding to $P_0 = 5 \text{ meV } \mu\text{m}^{-2}$ in the numerical modelling [38], the excitation k-vector plays a crucial role. Namely, since the point of inflexion of the lower polariton mode ($n = 0$) is at $\simeq 2.1 \mu\text{m}^{-1}$, polaritons excited by the pump in $n = 0$ have a negative effective mass. Hence, the interplay of the polariton GVD with the repulsive interactions can enable soliton formation [28]. Snap-shots of pulse evolution in real and momentum space are shown in Fig 3.

The initial pulse propagation is very similar to the case of the low power, P_1 , as can be seen by comparing panels (a) and (b) in Figs. 3 and 2. However, in contrast to the low power behaviour, here, at later times (50-80 ps), the polariton nonlinearity results in the emergence of a single dominant mode, when individual energy levels can no longer be resolved in the momentum space (Figs. 3(f,g), also Figs. S4(c-g,j-k) of the SM), which coincides with a significant narrowing of the pulse in real space (and hence in time) down to $\simeq 10 \mu\text{m}$, as in Fig. 3(c). The ratio between the peak intensities at 50-80 ps and 10 ps (Fig. 3(f-h)) is $\simeq 1.6$ times higher than the same ratio at low power (Figs. 2(f-h)). This is consistent with the concentration of pulse energy in the ground mode.

Kerr-like nonlinear interactions between transverse photonic modes in nonlinear crystals and optical fibres have been shown to lead to emergence of solitons and condensation of classical waves [8, 11]. A similar process occurs in the polariton MCW where polaritons, excited within a certain momentum (energy) range, populate other initially empty polariton states through nonlinear polariton-polariton scattering. In turn, this maximises the population of the ground mode $n = 0$ in the range of high momenta ($k \sim 2\text{-}2.5 \mu\text{m}^{-1}$). The interplay between negative polariton mass and nonlinear repulsive interactions between polaritons with different momenta in the ground mode leads to self-focusing and evolution of the system towards a temporal soliton at 50-75 ps. Some of the corresponding scattering channels are depicted in Fig. 4(a): interactions between polaritons residing initially in modes $n = 1$ and 2 result in a drastic increase of occupation in mode $n = 0$ as well as the occupation of higher order modes ($n = 3, 4$, and 5). Furthermore, both inter-modal and intra-modal scattering spreads polariton population over a large range of k-vectors, thus minimising peak intensities in momentum space of the excited transverse ($n \geq 1$) modes relative to the solitonic emission at $n = 0$. Note that the polariton population (and hence nonlinearity) diminishes with time due to the finite lifetime, which together with the GVD leads to broadening of the wavepacket at later times (> 75 ps). The experimental results in Fig. 3(f-h) are reproduced by the numerical modelling only when we include coherent interactions between multiple transverse modes (see Fig. S4 of the SM [38]).

The soliton regime described above does not correspond to a thermalised state, which is not achievable at the intermediate excitation power due to the finite polariton lifetime. However, at a higher excitation power, thermalisation can speed up due to the increased rate of polariton-polariton scattering. At $P_3 = 800 \mu\text{W}$, corresponding to $P_0 = 7 \text{ meV } \mu\text{m}^{-2}$ in the numerical modelling [38], a soliton doublet [29], corresponding to the soliton fission regime, emerges already at 10-15 ps after the excitation and remains stable until $\simeq 75$ ps (Figs. 5(b,c)). By 30-40 ps the emission follows the k_y

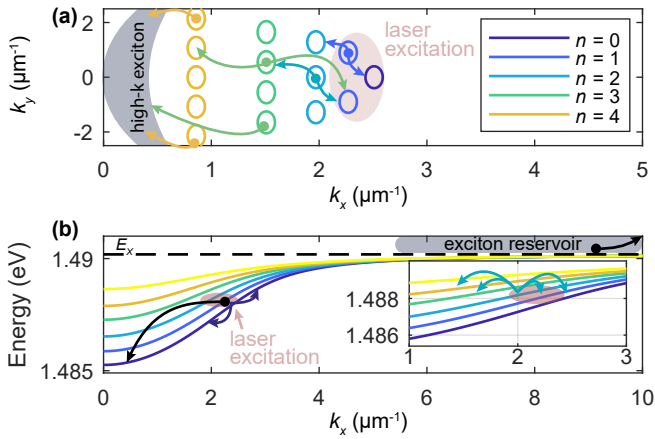


FIG. 4. (a) Schematic of some of the possible combinations for *inter-modal* polariton scattering in k -space at a fixed energy ($\simeq 1.488$ eV); the coloured ovals approximate location and width of different lower polariton energy modes; (b) Schematic of *intra-modal* polariton-polariton and polariton-exciton scattering leading to polariton relaxation. The inset corresponds to *inter-modal* scattering shown in (a).

profile of the ground mode, with a single antinode, and has the broad modulated spectrum arising from broadband inter- and intra-modal polariton-polariton scattering (modulation instability) as can be seen in Figs. 5(h,i). A large part of the the soliton doublet spectrum now lies below the point of inflexion (at $k_x \simeq 1.8 \mu\text{m}^{-1}$), in the region where polariton effective mass is positive, and where wavepacket defocusing is expected. In this case, solitons can give up their energy to extended dispersive modes with lower k -vectors via Cherenkov radiation [39, 46, 47]. From a microscopical point of view, this process again can be understood as a result of multiple polariton-polariton scattering events. During each of these, a pair of polaritons of the same energy scatter one to a lower and the second to a higher energy state. This mechanism results in a gradual shift of the maximum of the polariton distribution to lower k -vectors since the high-energy, high- k polaritons experience greater losses due to scattering to high-density high-momenta exciton-like states, the so-called exciton reservoir [48]. The losses may arise from interaction of polaritons with excitonic disorder [49, 50] or polariton-phonon and polariton-electron scattering [51]. The mechanisms involving the reservoir are not directly taken into account in our numerical modelling (which reproduces experimental results well, see Figs. S5 of the SM [38]), but are accounted for phenomenologically by introducing excitonic decay rates higher than photonic. Furthermore, even though the energy of the lower polariton states is below that of bare uncoupled excitons, coherent pair polariton-polariton scattering may also effectively populate the latter mainly due to a very high density of exciton states (Fig. 4(a)). This is confirmed by our simulations (see Figs. S5(j-l) of the SM [38]). Finally,

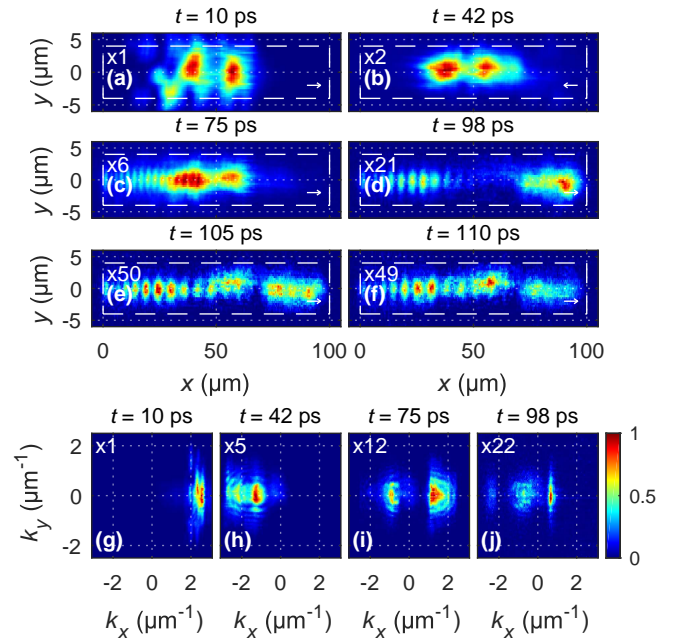


FIG. 5. High power, $P_3 = 800 \mu\text{W}$, emission characterisation for different times. (a-f) Reconstructed real-space images of the polariton pulse propagating in the MCW at different times. White dashed rectangles show the outline of the MCW. Arrows in lower right corners indicate the direction of travel of the pulses. (g-j) are the corresponding snapshots of the momentum space at the same times as (a-d) respectively. All pseudo-colour scales are linear 0 to 1, and numbers in top-right corners of each panel are intensity scaling factors applied to data for each panel.

note that polariton scattering with high-momenta excitons shown in Fig. 4(b) probably also plays an important role in the polariton relaxation [52]. Therefore, a number of mechanisms are potentially involved in spectral redistribution of polaritons in the wavepacket.

At $\simeq 75$ ps slow counter propagating waves emerge in the wire at $k_x \simeq \pm 0.8-1 \mu\text{m}^{-1}$ leading to formation of a modulated tail behind the doublet. At $\simeq 100$ ps the polariton emission mostly peaks at $k_x \simeq 0.5-0.7 \mu\text{m}^{-1}$, lower than the momentum of the excitation pulse. This corresponds to onset of a standing wave with 17 maxima seen in Figs. 5(d-f). The same effect is also observed in our modelling in Figs. S5(d,h,j) of the SM [38]. This standing wave arises from the interference across the whole wire between two waves at $k_x \simeq \pm 0.5-0.6 \mu\text{m}^{-1}$ which are long-range and coherent and hence form a macroscopically occupied state (a dynamic analogue of a nonequilibrium BEC).

Discussion. — Our findings show that in a sample with a long polariton lifetime, condensates can emerge out of a resonantly excited polariton cloud. By varying the energy, bandwidth, and power of the excitation pulse it is possible to control the excited polariton modes and their energy-momentum distributions. Resonant excita-

tion can also allow control of the spin degree of freedom, which can be useful for investigation of BKT phases [53] associated with the emergence of half- or full-spin vortex excitations in polariton systems with spin-anisotropic interactions [54], so far a completely unexplored field.

All our experimental observations are qualitatively reproduced by our numerical modelling. This shows that the condensation arises fundamentally from the very strong nonlinear response in the generalised Gross-Pitaevskii equation used to describe the polariton system. While we employ direct numerical integration, wave turbulence theories have been applied to a wide variety of GPE-type systems to explain classical condensation as irreversible evolution to a thermodynamic equilibrium state [10]. In 3D, condensation to either soliton [55] or CW [11] states has been studied for focussing or defocussing conditions respectively. Condensation was also shown theoretically for nonlocal and saturable nonlinearities and defocussing 2D and multimode waveguide systems [10]. The microcavity polariton dispersion provides a transition from focussing to defocussing as the mass changes sign and we observe the transition from solitonic to condensate final state with increasing density, even though the pump always corresponds to focussing conditions. An interesting experimental and theoretical perspective would be to study the equilibrium state of systems with this dispersion. We note also that one can extend theories to account for the couplings to phonon and exciton reservoirs present in polariton systems using kinetic Boltzmann [56] or stochastic GPE [57] approaches.

Acknowledgements. — MS and DNK acknowledge support from the Leverhulme Trust grant No. RPG-2013-339. MS, JKC, PMW, BR, MSS, and DNK acknowledge the support from the EPSRC grants EP/J007544/1, EP/N031776/1, and the ERC Advanced Grant EX-CIPOL 320570. DVS acknowledges Russian Foundation for Basic Research (16-52-150006); ITMO University Fellowship through the Government of Russia grant 074-U01. HS and IAS acknowledge the support by the Research Fund of the University of Iceland, The Icelandic Research Fund, Grant No. 163082-051 and the Project 3.2614.2017/4.6 of the Ministry of Education and Science of Russian Federation. IAS, MSS and DNK from Megagrant No. 14.Y26.31.0015 of the Ministry of Education and Science of Russian Federation.

We thank Marzena Szymańska for helpful discussions.

* m.sich@sheffield.ac.uk

† d.krizhanovskii@sheffield.ac.uk

- [1] N. P. Proukakis, D. W. Snoke, and P. B. Littlewood, eds., *Universal themes of Bose-Einstein condensation* (Cambridge University Press, 2017) p. 649.
 [2] C. E. Whittaker, B. Dzurak, O. A. Egorov, G. Buon-

- aiuto, P. M. Walker, E. Cancellieri, D. M. Whittaker, E. Clarke, S. S. Gavrilov, M. S. Skolnick, and D. N. Krizhanovskii, *Physical Review X* **7**, 031033 (2017).
 [3] Y. S. Kivshar and G. P. Agrawal, *Optical Solitons*, 1st ed. (Academic Press, 2003).
 [4] L. Khaykovich, F. Schreck, G. Ferrari, T. Bourdel, J. Cubizolles, L. D. Carr, Y. Castin, and C. Salomon, *Science* **296**, 1290 (2002).
 [5] K. E. Strecker, G. B. Partridge, A. G. Truscott, and R. G. Hulet, *Nature* **417**, 150 (2002).
 [6] M. Sich, D. V. Skryabin, and D. N. Krizhanovskii, *Comptes Rendus Physique* **17**, 908 (2016).
 [7] L. G. Wright, S. Wabnitz, D. Christodoulides, and F. W. Wise, *Physical Review Letters* **115**, 223902 (2015).
 [8] C. Sun, S. Jia, C. Barsi, S. Rica, A. Picozzi, and J. W. Fleischer, *Nature Physics* **8**, 470 (2012).
 [9] K. Krupa, A. Tonello, A. Barthélémy, V. Couderc, B. M. Shalaby, A. Bendahmane, G. Millot, and S. Wabnitz, *Physical Review Letters* **116**, 183901 (2016).
 [10] A. Picozzi, J. Garnier, T. Hansson, P. Suret, S. Randoux, G. Millot, and D. N. Christodoulides, *Physics Reports* **542**, 1 (2014).
 [11] C. Connaughton, C. Josserand, A. Picozzi, Y. Pomeau, and S. Rica, *Physical Review Letters* **95**, 263901 (2005).
 [12] B. Barviau, B. Kibler, A. Kudlinski, A. Mussot, G. Millot, and A. Picozzi, *Optics Express* **17**, 7392 (2009).
 [13] A. Picozzi, S. Pitois, and G. Millot, *Physical Review Letters* **101**, 093901 (2008).
 [14] A. V. Gorbach and D. V. Skryabin, *Optics Letters* **31**, 3309 (2006).
 [15] D. Snoke, G. Liu, and S. Girvin, *Annals of Physics* **327**, 1825 (2012).
 [16] F. Poletti and P. Horak, *Journal of the Optical Society of America B* **25**, 1645 (2008).
 [17] A. A. Sukhorukov, A. Ankiewicz, and N. N. Akhmediev, *Optics Communications* **195**, 293 (2001).
 [18] N. A. Gippius, I. A. Shelykh, D. D. Solnyshkov, S. S. Gavrilov, Y. G. Rubo, A. V. Kavokin, S. G. Tikhodeev, and G. Malpuech, *Physical Review Letters* **98**, 236401 (2007).
 [19] P. M. Walker, L. Tinkler, D. V. Skryabin, A. Yulin, B. Royall, I. Farrer, D. A. Ritchie, M. S. Skolnick, and D. N. Krizhanovskii, *Nature Communications* **6**, 8317 (2015).
 [20] J. Kasprzak, M. Richard, S. Kundermann, A. Baas, P. Jeambrun, J. M. J. Keeling, F. M. Marchetti, M. H. Szymańska, R. André, J. L. Staehli, V. Savona, P. B. Littlewood, B. Deveaud, and L. S. Dang, *Nature* **443**, 409 (2006).
 [21] M. Galbiati, L. Ferrier, D. D. Solnyshkov, D. Tanese, E. Wertz, A. Amo, M. Abbarchi, P. Senellart, I. Sagnes, A. Lemaître, E. Galopin, G. Malpuech, and J. Bloch, *Physical Review Letters* **108**, 126403 (2012).
 [22] D. Bajoni, P. Senellart, E. Wertz, I. Sagnes, A. Miard, A. Lemaître, and J. Bloch, *Physical Review Letters* **100**, 047401 (2008).
 [23] Y. Sun, P. Wen, Y. Yoon, G. Liu, M. Steger, L. N. Pfeiffer, K. West, D. W. Snoke, and K. A. Nelson, *Physical Review Letters* **118**, 016602 (2017).
 [24] D. N. Krizhanovskii, S. S. Gavrilov, A. P. D. Love, D. Sanvitto, N. A. Gippius, S. G. Tikhodeev, V. D. Kulakovskii, D. M. Whittaker, M. S. Skolnick, and J. S. Roberts, *Physical Review B* **77**, 115336 (2008).
 [25] K. G. Lagoudakis, M. Wouters, M. Richard, A. Baas,

- I. Carusotto, R. Andre, L. S. Dang, and B. Deveaud-Pledran, *Nature Physics* **4**, 706 (2008).
- [26] G. Tosi, G. Christmann, N. G. Berloff, P. Tsotsis, T. Gao, Z. Hatzopoulos, P. G. Savvidis, and J. J. Baumberg, *Nature Communications* **3**, 1243 (2012).
- [27] A. Amo, S. Pigeon, D. Sanvitto, V. G. Sala, R. Hivet, I. Carusotto, F. Pisanello, G. Leménager, R. Houdré, E. Giacobino, C. Ciuti, and A. Bramati, *Science* **332**, 1167 (2011).
- [28] M. Sich, D. N. Krizhanovskii, M. S. Skolnick, A. V. Gorbach, R. Hartley, D. V. Skryabin, E. A. Cerda-Méndez, K. Biermann, R. Hey, and P. V. Santos, *Nature Photonics* **6**, 50 (2012).
- [29] J. K. Chana, M. Sich, F. Fras, A. V. Gorbach, D. V. Skryabin, E. Cancellieri, E. A. Cerda-Méndez, K. Biermann, R. Hey, P. V. Santos, M. S. Skolnick, and D. N. Krizhanovskii, *Physical Review Letters* **115**, 256401 (2015).
- [30] R. M. Stevenson, V. N. Astratov, M. S. Skolnick, D. M. Whittaker, M. Emam-Ismael, A. I. Tartakovskii, P. G. Savvidis, J. J. Baumberg, and J. S. Roberts, *Physical Review Letters* **85**, 3680 (2000).
- [31] L. Ferrier, E. Wertz, R. Johnne, D. D. Solnyshkov, P. Senellart, I. Sagnes, A. Lemaître, G. Malpuech, and J. Bloch, *Physical Review Letters* **106**, 126401 (2011).
- [32] E. Wertz, L. Ferrier, D. D. Solnyshkov, R. Johnne, D. Sanvitto, A. Lemaître, I. Sagnes, R. Grousson, A. V. Kavokin, P. Senellart, G. Malpuech, and J. Bloch, *Nature Physics* **6**, 860 (2010).
- [33] G. Dasbach, M. Schwab, M. Bayer, D. N. Krizhanovskii, and A. Forchel, *Physical Review B* **66**, 201201 (2002).
- [34] H. Sigurdsson, I. A. Shelykh, and T. C. H. Liew, *Physical Review B* **92**, 195409 (2015).
- [35] H. Sigurdsson, T. C. H. Liew, and I. A. Shelykh, *Physical Review B* **96**, 205406 (2017).
- [36] A. I. Tartakovskii, D. N. Krizhanovskii, and V. D. Kulakovskii, *Physical Review B* **62**, R13298 (2000).
- [37] I. Carusotto and C. Ciuti, *Physical Review Letters* **93**, 166401 (2004).
- [38] See Supplemental Material at [link] for details of numerical modelling of kinetic evolution of polariton wavepackets, which includes Refs. [37, 58–60].
- [39] D. V. Skryabin, Y. V. Kartashov, O. A. Egorov, M. Sich, J. K. Chana, L. E. Tapia Rodriguez, P. M. Walker, E. Clarke, B. Royall, M. S. Skolnick, and D. N. Krizhanovskii, *Nature Communications* **8**, 1554 (2017).
- [40] C. Antón, T. C. H. Liew, G. Tosi, M. D. Martín, T. Gao, Z. Hatzopoulos, P. S. Eldridge, P. G. Savvidis, and L. Viña, *Physical Review B* **88**, 035313 (2013).
- [41] D. V. Skryabin and A. V. Gorbach, *Reviews of Modern Physics* **82**, 1287 (2010).
- [42] S. K. Turitsyn, A. E. Bednyakova, M. P. Fedoruk, S. B. Papernyi, and W. R. Clements, *Nature Photonics* **9**, 608 (2015).
- [43] E. G. Turitsyna, G. Falkovich, A. El-Taher, X. Shu, P. Harper, and S. K. Turitsyn, *Physical Review A* **80**, 031804(R) (2009).
- [44] L. Tinkler, P. M. Walker, E. Clarke, D. N. Krizhanovskii, F. Bastiman, M. Durska, and M. S. Skolnick, *Applied Physics Letters* **106**, 021109 (2015).
- [45] Emission at small positive values of k_x ($\simeq +1.5 \mu\text{m}^{-1}$) relative to the magnitudes at $-k_x$ on panel (f) may be due to the effect of disorder scattering on reflection at the end of the MCW.
- [46] K. Hammani, B. Kibler, C. Finot, and A. Picozzi, *Physics Letters A* **374**, 3585 (2010).
- [47] D. V. Skryabin, F. Luan, J. C. Knight, and P. S. J. Russell, *Science* **301**, 1705 (2003).
- [48] P. M. Walker, L. Tinkler, B. Royall, D. V. Skryabin, I. Farrer, D. A. Ritchie, M. S. Skolnick, and D. N. Krizhanovskii, *Physical Review Letters* **119**, 097403 (2017).
- [49] D. N. Krizhanovskii, A. I. Tartakovskii, A. V. Chernenko, V. D. Kulakovskii, M. Emam-Ismael, M. S. Skolnick, and J. S. Roberts, *Solid State Communications* **118**, 583 (2001).
- [50] V. D. Kulakovskii, A. I. Tartakovskii, D. N. Krizhanovskii, M. S. Skolnick, and J. S. Roberts, *Physica E: Low-Dimensional Systems and Nanostructures* **13**, 455 (2002).
- [51] A. I. Tartakovskii, D. N. Krizhanovskii, G. Malpuech, M. Emam-Ismael, A. V. Chernenko, A. V. Kavokin, V. D. Kulakovskii, M. S. Skolnick, and J. S. Roberts, *Physical Review B* **67**, 165302 (2003).
- [52] P. G. Savvidis, J. J. Baumberg, D. Porras, D. M. Whittaker, M. S. Skolnick, and J. S. Roberts, *Physical Review B* **65**, 073309 (2002).
- [53] D. Caputo, D. Ballarini, G. Dagvadorj, C. S. Muñoz, M. De Giorgi, L. Dominici, K. West, L. Pfeiffer, G. Gigli, F. P. Laussy, M. H. Szymańska, and D. Sanvitto, *arXiv:1610.05737* (2016).
- [54] M. Vladimirova, S. Cronenberger, D. Scalbert, K. V. Kavokin, A. Miard, A. Lemaître, J. Bloch, D. Solnyshkov, G. Malpuech, and A. V. Kavokin, *Physical Review B* **82**, 075301 (2010).
- [55] R. Jordan and C. Jossierand, *Physical Review E* **61**, 1527 (2000).
- [56] I. G. Savenko, T. C. H. Liew, and I. A. Shelykh, *Physical Review Letters* **110**, 127402 (2013).
- [57] M. Wouters, T. C. H. Liew, and V. Savona, *Physical Review B* **82**, 245315 (2010).
- [58] V. Savona, *Journal of Physics: Condensed Matter* **19**, 295208 (2007).
- [59] F. Baboux, L. Ge, T. Jacqmin, M. Biondi, E. Galopin, A. Lemaître, L. Le Gratiet, I. Sagnes, S. Schmidt, H. E. Türeci, A. Amo, and J. Bloch, *Physical Review Letters* **116**, 066402 (2016).
- [60] W. Pauli, *Wave Mechanics: Volume 5 of Pauli Lectures on Physics* (Dover Publications, 2000) p. 240.